Third International Conference on Sustainable Construction Materials and Technologies http://www.claisse.info/Proceedings.htm

Performance of ternary blended cement systems suitable for ultrahigh strength concrete

Kanako MORI[1] , Katsuya KONO[1] and Shunsuke HANEHARA[2]

[1]Taiheiyo Cement Corporation, 2-4-2, Osaku, Sakura-shi, Chiba-ken, Japan.
<Kanako_Mori@taiheiyo-cement.co.jp>, <Katsuya_Kono@taiheiyo-cement.co.jp>
[2] IWATE University, 4-3-5, Ueda, Morioka-shi, Iwate-ken, Japan
<hanehara@iwate-u.ac.jp>

ABSTRACT

To achieve high fluidity and compressive strength in ternary blended cement systems for ultrahigh strength concrete, particle composition and the influence of curing temperature on hardened mortar were examined. As a result, the flow value of fresh mortar and the compressive strength of hardened mortar were increased but no influence on hydration was observable when the BET specific surface of silica fume (SF) was changed from 20 m^2/g to 10 m^2/g. When mortar including cement systems consisted of 60 vol.% of moderate heat Portland cement, 20 vol.% of silica fine powder and 20 vol.% of SF with a BET specific surface of 10 m^2/g, it provided high performance, but the particle composition included more intermediate particles than the amount calculated according to theory of closest packing density. Furthermore, the pozzolanic reaction was accelerated as curing temperature increased.

Keywords. Fluidity, Porosity, Silica fume, Ternary blended cement, Ultrahigh strength concrete.

INTRODUCTION

Improvement of durability of concrete can make concrete structures resistant, makes maintenance easy, and extends their life cycle. High durability and high strength of concrete structures may contribute to the achievement of sustainability in construction. Recently, ultrahigh strength concrete with more than 200 MPa compressive strength has been developed. This concrete is manufactured by mixing cement with silica fume at a water-cement ratio (W/C) of less than 20 mass%. Concrete compressive strength mixed at a lower W/C increases. However, using superplasticizer and adjusting the particle distribution of the cement system are inevitable in order to mix cement at a lower W/C.

Ultrahigh strength cement systems can be applied to ultrahigh strength fiber reinforced concrete (UFC). UFC needs standard heat curing, which is curing at 90°C for 48 hours according to "Recommendations for Design and Construction of Ultrahigh Strength Fiber Reinforced Concrete Structures, -Draft" (JSCE, 2004). Standard heat curing promotes high density of UFC mass, provides the internal development of high strength, and improves durability. Meanwhile, increasing curing temperature and curing time causes an increase in

manufacturing cost and decrease in productivity. Therefore, it is important to understand the relationship in the hardened concrete between performance and curing conditions.

In this study, the effects of particle distribution of cement systems and curing conditions on the fluidity of fresh mortar were examined. Compressive strength, porosity and content of combined water and $Ca(OH)_2$ of hardened mortar were also investigated.

EXPERIMENT

Materials and mix proportions

Materials used in this study are shown in Table 1. Moderate heat Portland cement (MHC) was used for the base cement. Ternary blended cement was produced by mixing MHC as the coarse grain, silica fume (SF) as the fine grain and silica fine powder (SI) as the intermediate grain. Grain size distribution of particles is shown in Fig. 1. Two different SF types were prepared to determine the effect of their BET specific surface. LSF is ten times the size of HSF. The fine aggregate and polycarboxylate superplasticizer (SP) used were standard materials for UFC.

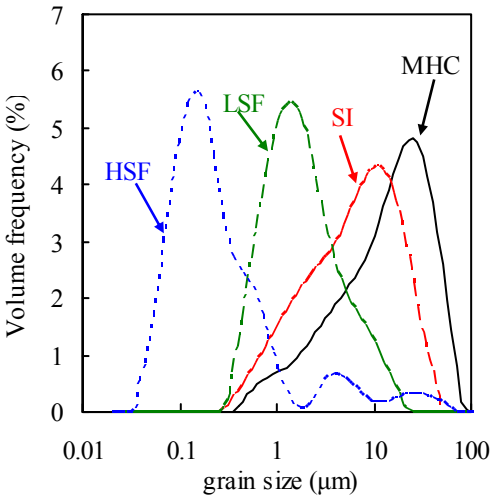

Fig. 1. Grain size distribution of particles

The amount of fine aggregate and SP were fixed for every mortar mix. Fine aggregate was 362 l/m^3 and SP was PM x 2.5 mass%. Mixing proportions of blends are listed in Table 2. Ternary blended cement systems were composed within the limits of 40 to 80 vol.% of MHC, 10 to 40 vol.% of SF and 0 to 40 vol.% of SI. Furthermore, the water-powder ratio (W/PM) was within the limit of 38 to 42 vol.%.

Table 1. Properties of materials used

Material		Symbol			Remarks	Density (g/cm^3)	Average particle size (μm)
Premixed powder	Cement	PM	MHC		Moderate heat Portland cement	3.21	20
	Silica fume		SF	LSF	BET specific surface 10 m^2/g	2.40	1.3
				HSF	BET specific surface 20 m^2/g	2.20	0.1
	Silica fine powder		SI		Blaine fineness 7500 m^2/kg	2.67	7.2
Fine aggregate		S			Silica sand under 2.5 mm	2.61	-
Admixture		SP			Polycarboxylate superplasticizer	-	-

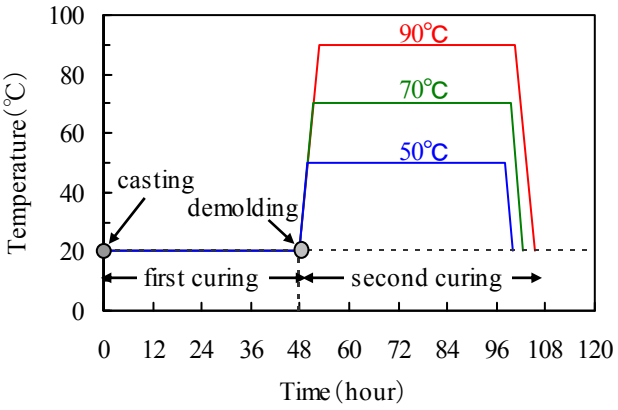

Fig. 2. Conditions of heat curing

Table 2. Mixture proportions

SF types	W/PM (vol.%)	Particle distribution (vol.%)		
		MHC	SF	SI
LSF	40	80	20	0
		80	10	10
		70	20	10
		70	10	20
		60	30	10
		60	20	20
		60	10	30
		50	40	10
		50	30	20
		50	20	30
		50	10	40
		40	40	20
		40	30	30
		40	20	40
	38	60	30	10
		60	20	20
		50	30	20
		40	30	30
		40	20	40
HSF	42	80	20	0
		60	30	10
		60	20	20
		60	10	30
		50	30	20
		40	30	30
		40	20	40

Experimental method

Determining the fluidity of fresh mortar is generally done according to JIS 5201, which states that the flow should be measured after removing the flow cone and performing 15 hits. However, for the purposes of UFC, this method was modified such that the flow is measured after 180 seconds with no hits. Secondly, to examine the properties of hardened mortar, compressive strength, porosity and contents of combined water and $Ca(OH)_2$ were measured from a selection of mixture proportions. Compressive strength was measured with ϕ5 x 10 cm specimens in accordance with JSCE-G505-1999. Pore size distribution was measured with a mercury-intrusion porosimeter within the limits of 3 nm to 400 μm. The combined water and $Ca(OH)_2$ were determined by the ignition loss method at 1000°C and thermogravimetry (TG) – differential scanning calorimetry (DSC), respectively. Furthermore, premixed powder was observed via scanning electron microscope (SEM) and optical microscope. All samples, except for the premixed powder and the specimens for compressive strength measurement, were immersed in acetone to terminate hydration.

Heat curing

To evaluate the effect of curing conditions on the properties of hardened mortar, curing was conducted at several different maximum temperatures: 90 °C, 70 °C and 50 °C. Conditions of heat curing are shown in Fig. 2. The specimens were demolded after 48 hours at 20 °C with sealed condition (first curing), then put into steam curing for 48 hours at each temperature (second curing). The heating and cooling speed was fixed. In addition, to observe the effect of the heat curing, some samples were simply left at 20 °C and their properties were compared with the heat curing samples.

Theory of closest packing

Furnas addressed in his work the closest packing of particles when there are two to four particle types (Furnas, 1931). The theory of closest packing states that the holes between the larger particles are filled with smaller particles, whose voids in turn are filled with smaller ones, and so on until the smallest particles. According to his study, the ratio between the size of the smallest and largest particles, which is defined as *K*, decides how many components fit together in closest packing. The relationship between the number of components for closest packing (system of maximum density) and *K* is shown in Fig. 3.

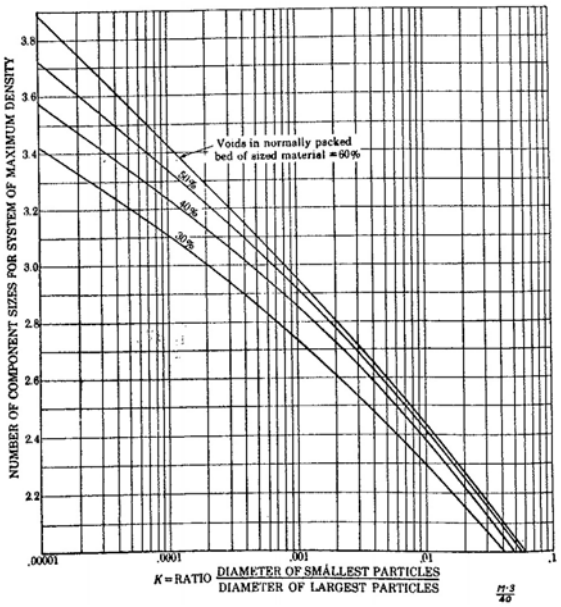

Fig. 3. Relation between size ratio and number of component sizes for systems of maximum density (Furnas, 1931)

In this study, the powder composition for maximum packing density was calculated according to Furnas' theory. Average size and density of particles are shown in Table 1. Voids ratio, which is the fraction of voids in a bed of a given size, is assumed to be 0.50. *K* between MHC and LSF is 1.3 μm / 20 μm = 6.5 x 10^{-2} so the number of components for closest packing is two. Meanwhile, *K* between MHC and HSF is 0.1 μm / 14 μm = 5.0 x 10^{-3} so the number of components for closest packing is three. Powder composition is given by the following equations.

$$\text{Total weight} = W_1 + 1 - W_1 + (1 - W_1) \{ (1 - W_2) / W_2 \} \quad (1)$$

$$\text{where} \quad W_1 = (1 - V_1) S_1 / \{ (1 - V_1) S_1 + V_1 (1 - V_2) S_2 \} \quad (2)$$

$$W_2 = (1 - V_2) S_2 / \{ (1 - V_2) S_2 + V_2 (1 - V_3) S_3 \} \quad (3)$$

where V_1 is voids in MHC, V_2 is voids in SI or LSF, V_3 is voids in HSF, S_1 is density of MHC, S_2 is density of SI or LSF, and S_3 is density of HSF.

Thus, powder composition for closest packing was determined to be 80 vol.% of MHC and 20 vol.% of LSF when PM includes LSF. On the other hand, it is 60 vol.% of MHC, 30 vol.% of SI and 10 vol.% of HSF when PM includes HSF.

RESULTS AND DISCUSSION

Fluidity

The flow value of mortar including LSF at W/PM 40 vol.% (14 mass%) is shown in Fig. 4. The figure reveals that fluidity is extremely different according to the powder composition. The circle in the figure shows the combination of powder to achieve high fluidity. On the other hand, in the case of the powder composition within 70 to 80 vol.% of MHC and 10 vol.% of LSF, the flow value significantly decreased. Incidentally, the powder composition of closest packing according to Furnas' theory is with 80 vol.% of MHC and 20 vol.% of

LSF, but flow value of that composition is 192 mm. Therefore, it was revealed that the powder composition of maximum packing density calculated according to theory had little correlation with the powder composition of the best flow value, because the flow value within the circle in Fig. 4 was more than 300 mm. It was found that the intermediate particles in the powder to obtain high fluidity and high compressive strength were slightly increased compared to closest packing density. This is consistent with a previous study that showed that cement suitable for high strength concrete is made of the base cement as the intermediate grain, recycled grain of MHC in finishing grinding as the coarse grain and limestone powder as the fine particles (Uchikawa *et al*., 1995).

The flow value of mortar including LSF at W/PM 38 vol.% (13 mass%) is shown in Fig. 5. The numbers of the powder composition to achieve high fluidity were decreased because W/PM was 2 vol.% lower. However, W/PM may be lower than 38 vol.% at the powder composition within the circle in Fig. 5 because its flow value decreased slightly, particularly for 60 vol.% of MHC, 20 vol.% of SI and 20 vol.% of LSF.

The flow value of mortar including HSF at W/PM 42 vol.% (14 mass%) is shown in Fig. 6. This result revealed that HSF made the fluidity of fresh mortar lower than LSF. The flow value was significantly decreased, especially when HSF was more than 30 vol.% and SI was less than 10 vol.%. On the other hand, the flow value increased when the content of MHC was decreased and the content of SI was increased. This result was consistent with PM including LSF. Furthermore, the powder composition which yielded the best flow had little correlation to the one calculated by Furnas' theory. This observation was also found in PM including LSF.

Observation of premixed powder

Premixed powder before hydration was observed with SEM. Samples were immersed

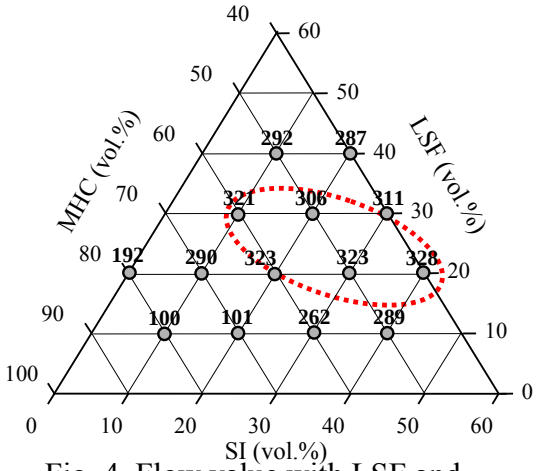

Fig. 4. Flow value with LSF and W/PM 40 vol. %

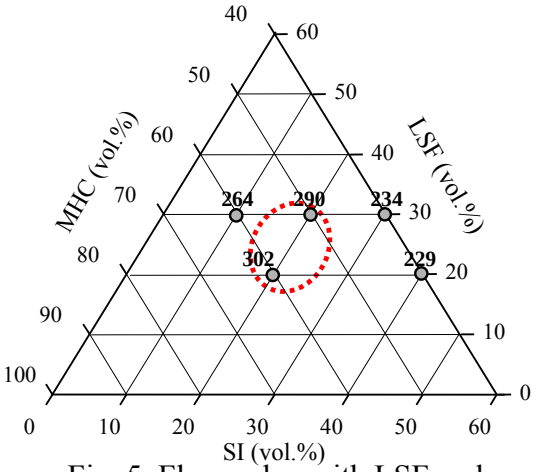

Fig. 5. Flow value with LSF and W/PM=38 vol. %

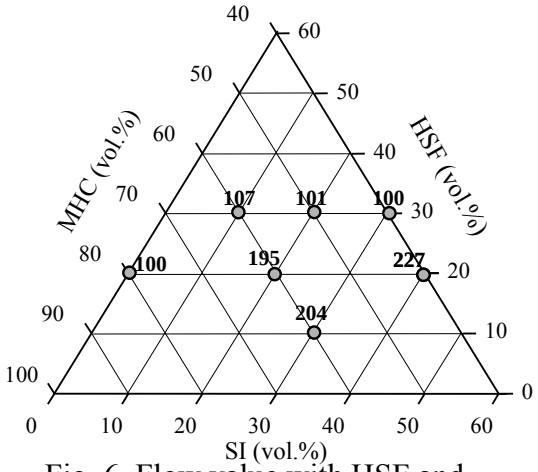

Fig. 6. Flow value with HSF and W/PM=42 vol. %

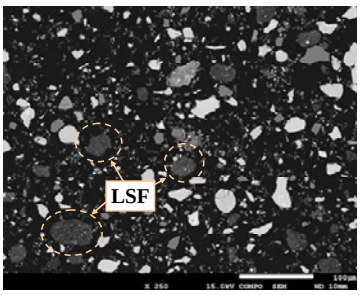

Fig. 7. PM including LSF

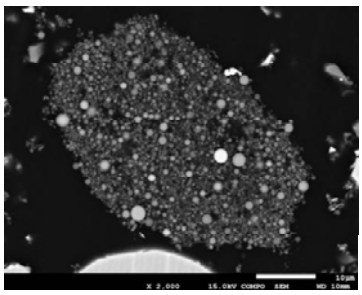

Fig. 8. Agglomeration of LSF

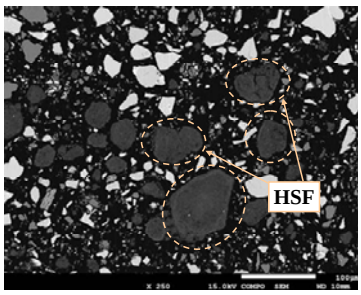

Fig. 9. PM including HSF

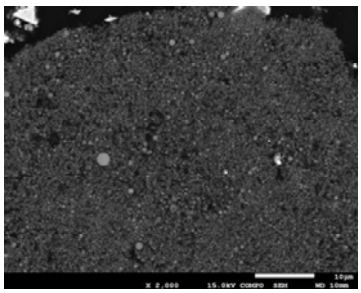

Fig. 10. Agglomeration of HSF

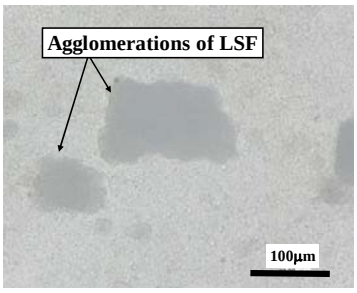

Fig. 11. Agglomeration of LSF in SP

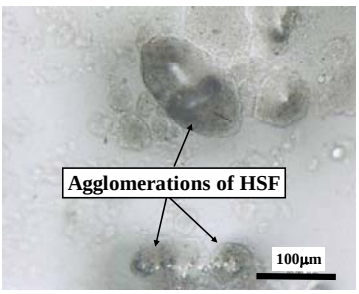

Fig. 12. Agglomeration of HSF in SP

in resin and polished. Fig. 7 and Fig. 8 present SEM images of PM including LSF. On the other hand, Fig. 9 and Fig. 10 present SEM images of PM including HSF. These SEM images show that particles of MHC and SI were spread independently, but particles of SF were agglomerated. Particularly, the agglomeration size of HSF seemed to be bigger than that of LSF.

Particles of SF mixed in polycarboxylate superplasticizer were observed via optical microscope. Images of LSF and HSF are shown in Fig. 11 and Fig. 12, respectively. These images suggested that polycarboxylate superplasticizer can't spread SF particles perfectly. Therefore, the average particle was 1.3 μm for LSF and 0.1 μm for HSF when the grain size distribution of particles was measured with dispersant and ultrasound (Fig. 1). However, SF may form lumps of particles in premixed powder and mortar. Furthermore, PM including HSF may have more lumps of particles over 10 μm than PM including LSF.

Compressive strength

(1) Influence of W/PM and powder composition

Compressive strength of hardened mortar specimens mixed including LSF at W/PM 40 vol.%, LSF at W/PM 38 vol.% and HSF at W/PM 42 vol.% are shown in Fig. 13, Fig. 14, and Fig. 15 respectively. In Fig. 13, the case of LSF at W/PM 40 vol.%, the compressive strength of hardened mortar tended to decrease when PM included less than 10 vol.% of LSF but increased slightly when the amount of LSF included in PM was changed from 20 vol.% through 30 vol.% to 40 vol.%. In Fig. 14, the case of LSF at W/PM 38 vol.%, the compressive strength of hardened mortar was not significantly different. Fig. 13 and Fig. 14 suggest that the increase in compressive strength of hardened mortar mixed at the same powder composition is caused by the decrease of W/PM. In particular, improvement of the compressive strength of hardened mortar with decrease of W/PM was achieved when the powder composition was 60 vol.% of MHC, 20 vol.% of SI and 20 vol.% of LSF. Fig. 15

shows that the compressive strength of hardened mortar including HSF was lower than hardened mortar including LSF.

(2) Influence of curing temperature and SF types

The effect of curing temperature on compressive strength of hardened mortar when the powder composition was 60 vol.% of MHC, 20 vol.% of SI and 20 vol.% of SF is shown in Table 3. The results of the compressive strength of hardened mortar including HSF and cured at 90°C is also shown in Table 3 to determine the effect of SF types on compressive strength. W/PM was 40 vol.% and PM x 2.5 mass% in this experimental test. Table 3 shows the compressive strength of hardened mortar including LSF and cured at more than 50°C. The highest compressive strength of hardened mortar was approximately 200 MPa and it was obtained at 90°C heat curing. While the compressive strength of hardened mortar cured at between 50°C and 70°C showed almost no difference, the strength of the mortar cured at 20°C for 96 hours (LSF-20-2d) was approximately 100 MPa. Although this result shows that heat curing improves the compressive strength of hardened mortar, if the curing time at 20°C is longer, the compressive strength of hardened mortar can be improved because the strength of hardened mortar cured at 20°C for 168 hours (LSF-20-5d) was 130 MPa. These results suggest that heat curing at 90°C for several days is needed to obtain compressive strength over 200 MPa. However, the compressive strength of hardened mortar including HSF did not reach 200 MPa in spite of heat curing at 90°C.

Pore size distribution and porosity

The pore size distribution of the hardened mortars in Table 3 is shown in Fig. 16. The heat curing caused micro pores of 3nm to 6nm to increase and caused the total porosity to decrease significantly to less than

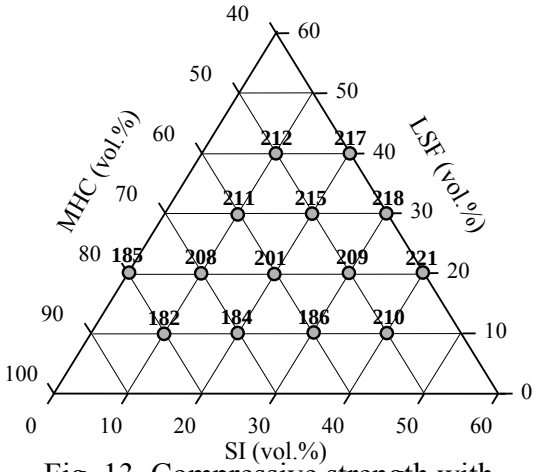

Fig. 13. Compressive strength with LSF and W/PM 40 vol. %

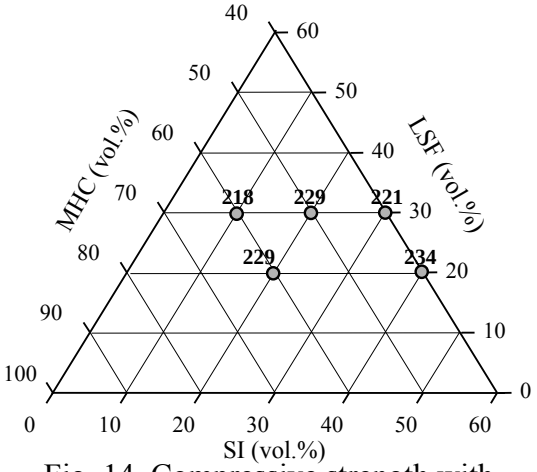

Fig. 14. Compressive strength with LSF and W/PM 38 vol. %

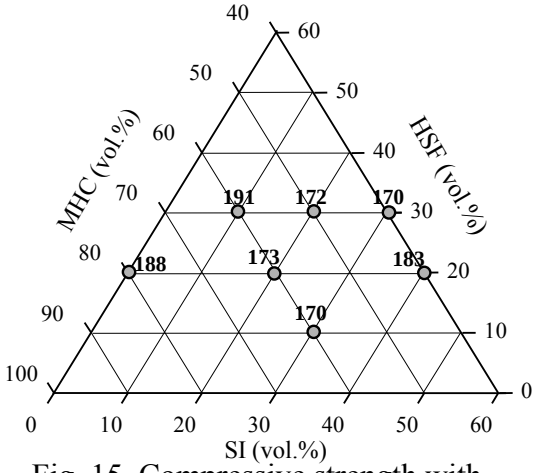

Fig. 15. Compressive strength with LSF and W/PM 42 vol. %

Table 3. Compressive strength with different curing conditions and SF

Symbol	SF types	W/PM (vol.%)	Composite (vol.%)			First curing		Second curing		Compressive strength (MPa)
			C	SF	SI	TEMP (°C)	Time (hour)	TEMP (°C)	Time (hour)	
LSF-90	LSF	40	60	20	20	20	48	90	48	201
LSF-70								70		184
LSF-50								50		181
LSF-20-2d								20		106
LSF-20-5d								20	120	130
HSF-90	HSF							90	48	176

4%. The results of hardened mortar including LSF revealed that the porosity of mortar, especially the pore size of 11nm to 100nm, was decreased with increasing heat curing temperature.

These results were also obtained when the term of curing at 20°C was longer.

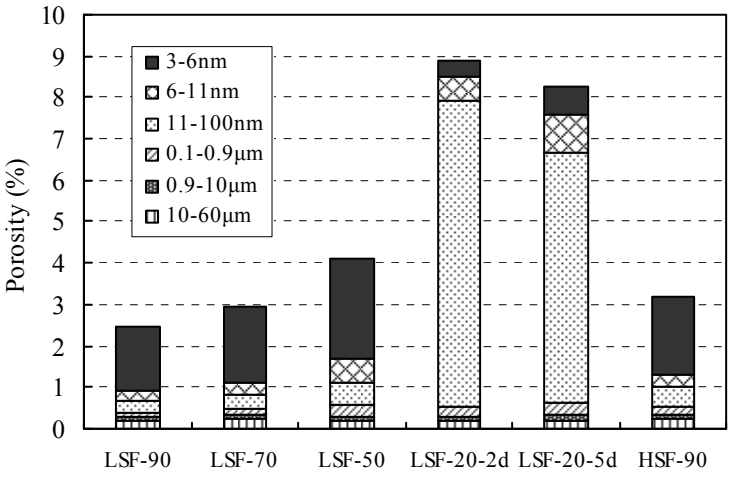

Fig. 16. Porosity with different curing conditions

Although the porosity of HSF-90 decreased, it was higher than the porosity of LSF-90. This may affect the difference in compressive strength. The relationship between the compressive strength and the degree of porosity is shown in Fig. 17. The figure revealed that the compressive strength increased with decreasing porosity, despite the differences in SF and curing conditions

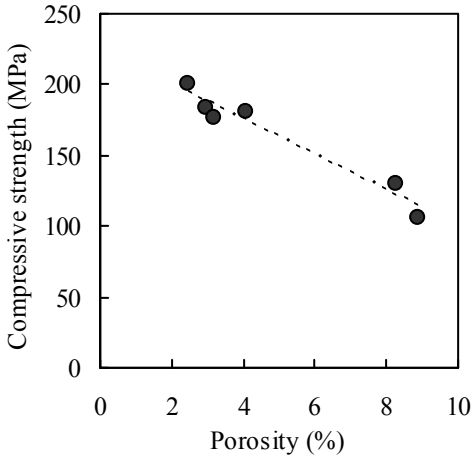

Fig. 17. Compressive strength versus porosity

Contents of combined water and of $Ca(OH)_2$ in hardened mortar

The contents of combined water and $Ca(OH)_2$ in hardened mortar are shown in Fig. 18. In the hardened mortar including LSF, the content of combined water was higher and that of $Ca(OH)_2$ was lower as curing temperature increased. This suggests that the pozzolanic reaction is accelerated by heat curing and correlated with temperature. Meanwhile, the contents of combined water and $Ca(OH)_2$ of HSF-90 were equal to those of LSF-90. This suggests that SF types do not affect the pozzolanic reaction.

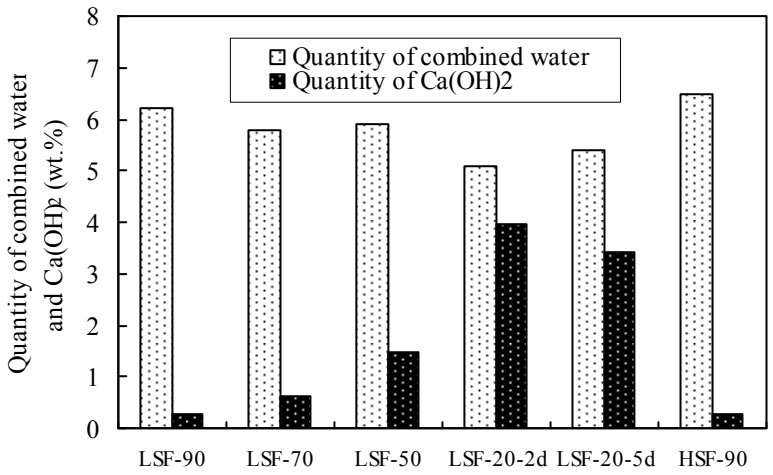

Fig. 18. Contents of combined water and $Ca(OH)_2$

CONCLUSION

In this study, the effects of particle distribution of cement systems and curing conditions on the fluidity of fresh mortar were examined. Compressive strength, porosity and content of combined water and $Ca(OH)_2$ of hardened mortar were also examined. The results obtained are as follows.

(1) The flow value of fresh mortar including cement systems composed of moderate heat Portland cement (MHC), silica fume (SF) and silica fine powder (SI) increased when the BET specific surface of SF was changed from 20 m^2/g to 10 m^2/g.

(2) High fluidity of fresh mortar was maintained and the compressive strength of hardened mortar was increased in spite of the water-powder ratio decreasing when cement systems composed of 60 vol.% of MHC, 20 vol.% of SI, and 20 vol.% of SF which had 10 m^2/g BET specific surface.

(3) The flow value of fresh mortar increased when the ratio of intermediate particles was higher than that calculated according to the theory of closest packing density.

(4) The porosity and the content of $Ca(OH)_2$ in hardened mortar decreased as curing temperature increased. This suggests that the pozzolanic reaction is accelerated as curing temperature increases.

(5) The compressive strength and porosity of hardened mortar were different but the combined water and $Ca(OH)_2$ content showed little difference when the BET specific surface of SF was changed. Therefore, SF types may not influence hydration.

REFERENCES

C. C. Furnas (1931). "Grading Aggregates I-Mathematical Relations for Beds of Broken Solids of Maximum Density. " INDUSTRIAL AND ENGINEERING CHEMISTRY. Vol.23, No.9, 1052-1058

Japan Society of Civil Engineers (2004). Recommendations for Design and Construction of Ultrahigh Strength Fiber Reinforced Concrete Structures, -Draft."

Uchikawa, H., Hanehara, S. and Hirao, H. (1995). "Cement for High-Strength Concrete with

Superior Workability Prepared by Adjusting the Composition and Particle Size Distribution. "Journal of research of the Chichibu Onoda Cement Corporation. Vol.46, No.129, 48-55